The CLAS Start Counter

S. Taylor [a], S. Ahmad [d], J. Distelbrink [c], G. S. Mutchler [a], E. Smith [b], and T. Smith [c,e]

[a] *Rice University, Houston, TX 77251-1892, USA*

[b] *Thomas Jefferson National Accelerator Facility, Newport News, VA 23606, USA*

[c] *University of New Hampshire, Durham, NH 03824, USA*

[d] *Department of Radiology, Baylor College of Medicine, One Baylor Plaza, Houston, Texas 77030*

[e] *Present Address: MIT Bates Linear Accelerator Center, Middleton, MA 01949, USA*

Abstract

The design, construction, and performance of a hexagonal-nose-cone shaped plastic scintillation counter system is described. This "Start Counter" is used as part of the trigger and to measure event start times for photon beam running with CLAS in Hall B at the Thomas Jefferson National Accelerator Facility. The Start Counter is constructed of three 3-mm thick coupled paddle scintillators and achieves a software-corrected time resolution of 260 ps. Each coupled-paddle scintillator operated without appreciable sagging up to ∼1.2 MHz rate.

Preprint submitted to Elsevier Preprint *27 September 2000*

Contents

PACS:
Keywords: CLAS, plastic scintillator, time of flight, trigger

1 Overview of CLAS

The Continuous Electron Beam Accelerator Facility (CEBAF) at the Thomas Jefferson National Accelerator Facility currently delivers CW electron beam up to ≈6 GeV in energy. The machine can deliver electrons to three experimental areas (Halls A, B, C) at any multiple of one-fifth of the end point energy. The beam has a 2.004 ns bunch structure with an energy spread of $\Delta E/E \leq 10^{-4}$. Hall B contains the CEBAF Large Acceptance Spectrometer (CLAS)[1] and a tagged photon facility. CLAS is based on a multi-gap magnet with six superconducting coils, symmetrically arranged to generate an approximately toroidal field distribution. Each of the six sectors is instrumented with drift chambers to determine charged particle trajectories, scintillation counters for the measurement of time-of-flight (TOF) and for triggering during photon beam running, gas Čerenkov counters for electron identification and an electromagnetic calorimeter for electron, photon and neutron energy measurement and detection.

A photon beam with energy resolution of $\Delta E_\gamma/E_\gamma \approx 10^{-3}$ is provided by a photon tagging system upstream of the CLAS detector [2]. The tagger provides photons with energies between 0.2–0.95 of the incident electron energy. Three hundred eighty-four overlapping E counters subdivide this region into 767 energy bins. The timing of the radiating electron is provided by 61 T-counters, sized to give approximately equal counting rate over the range of detected energy. These counters have better than 150 ps resolution.

In order to identify particles by TOF it is necessary to determine the flight time of particles of known momenta through a known trajectory in CLAS. The time of interaction is obtained by determining the electron beam bucket that produced the event, and the TOF scintillators measure the time at the end of the trajectory. The TOF system is described elsewhere [3]. To correlate the interaction time in the target with the photon production time, a sub-nanosecond coincidence of the tagging spectrometer with a counter (the "Start Counter") at the target is needed. The Start Counter is a system of three thin scintillation counters surrounding the target. Their design, construction, and performance is described below.

2 Design

The Start Counter system provides a fast timing signal as an input to the CLAS trigger. The hardware time is used in coincidence with the tagger counters to reduce the accidental trigger rates. The time of interaction at the target must be determined in hardware to ±2 ns. The software-corrected time should result in a confidence interval between ± 1 ns for the interaction of greater than 99%, i.e. have tails outside of 1 ns for no more than 1% of the events. For a gaussian time distribution, this translates into a standard deviation σ of 388 ps. Thus the Start Counter signal in coincidence with the T-counter time allows good identification of the RF bucket that produced the hadronic interaction in the target. Comparison to the nearest RF time gives the start time of the particle trajectory to better than 25 ps.

The acceptance of the Start Counters subtends the same solid angle as the TOF counters, $7^\circ < \theta < 145^\circ$, $-29^\circ < \phi < 29^\circ$, for an extended cylindrical target 17 cm long and 4 cm in diameter. Here θ and ϕ are the polar and azimuthal angles, respectively, relative to the beam direction. The support structure of the counters is confined within the shadow of the Toroid coils of CLAS and is attached to a flange on the upstream end of the cryotarget. Both photomultiplier tubes (PMTs) are upstream beyond the maximum angle of acceptance (142° from the beam direction as measured from the center point of the target). PMTs cannot be placed downstream of the Start Counter because they would interfere with the small angle acceptance of the CLAS or be subjected to an intense and potentially damaging photon flux.

Thin scintillators are required to minimize the effects of multiple scattering. There are three main contributions to the multiple scattering: the LH2 target ($X_0 = 865$ cm for liquid hydrogen), the 1.5 mm thick carbon fiber beam pipe surrounding the target ($X_0 = 18.8$ cm), and the Start Counters ($X_0 = 42.5$ cm). To keep the multiple scattering angle due to the start counter below that generated by the target and beam pipe ($\sim$1.5 mrad), the Start Counter scintillators are 3 mm thick.

The requirement that both of the PMTs be on the upstream end of the Start Counter, so that the PMTs would not interfere with charged particles produced in the CLAS target or intercept beam halo down stream of the target, ruled out a conventional double-ended six-counter design. Attempts to build six double-ended scintillators using either conventional light guides or optical fibers to pipe the light from the downstream end back to the upstream position failed due to inadequate light transmission, excess mass in the CLAS acceptance volume, and excessively fragile glue joints. The light guides could not be rigidly attached and bent in the limited space available. This lead to the present coupled-paddle design [5]. In this design, adjacent paddles are mechanically joined at the nose end to form three double ended paddles covering all six sectors. The performance of the coupled paddle design was estimated using the Guide7[6] ray-tracing program on a flat model of the final paddle. A charged particle event was simulated in one leg (or the opposite leg) and the trajectories of ten thousand photons were tracked. When the event was in the same leg as the PMT the collection efficiency was 20%, when the event was introduced in the other leg, the collection efficiency was 8.5%. See [5] for

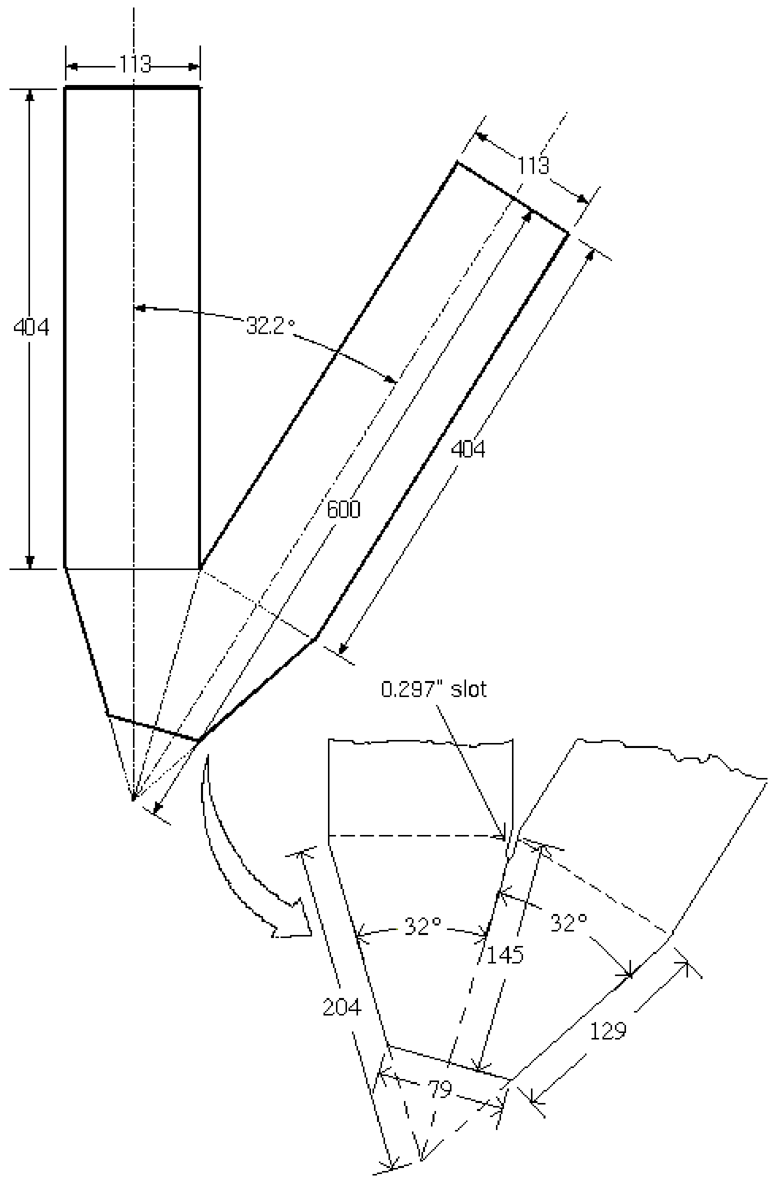

Fig. 1. Dimensions of each Start Counter scintillator. A detail of the nose region is also shown. All dimensions are in millimeters unless specified.

more details on the simulation.

3 Construction

The construction is described in detail in ref. [4]. Construction began with a flat sheet of scintillator as shown in figure 1. The scintillator was 3 mm thick

BC-408 [1] . The dimensions are given in the figure. The scintillator is bent at 60° along the centerline between the two legs. The legs are then bent through 30° to lie parallel to the target. The dashed lines in the figure show the positions of the bends. Three such counters then form a hexagonal-nose-cone structure surrounding the target. An XP-2262 2" PMT is attached to the end of each leg with an adiabatic light guide to form a double-ended paddle.

The scintillators were bent in three steps using a series of aluminum molds as shown in figure 2. The sides of the mold were covered with Kapton^{TM} tape and the flat surfaces of the mold were covered with a single smooth sheet of Mylar. Tests indicated that the softened scintillator would not adhere to Kapton^{TM} or Mylar. The mold was pre-heated to 70° C in an oven. Immediately after removing the mold from the oven, the scintillator was placed against the nose end of the mold and two pre-heated aluminum plates (coated with Kapton^{TM}) were placed on the scintillator with the region of the bend exposed. This region was then heated with a hand-held heat gun, until the scintillator softened. The heat gun was held approximately 6" from the scintillator to avoid localized overheating. As the softened scintillator bent, it was gently pushed into the mold. It was then lightly clamped into position and allowed to slowly cool. This procedure was repeated for each bend using the molds similar to that shown in figure 2. Great care is required to avoid over- or under-heating the scintillator. If the scintillator is bent before it is soft enough, it will tend to craze during cooling. If it is overheated, the edges will soften and become rounded. This will adversely effect the optics of the finished product. Finally, severe overheating will damage the scintillator. It is essential to develop a "feel" for this procedure by practicing with scraps of scintillator. The bent scintillator tends to develop a stress fracture at the mid-line of the joint between the two legs. A 0.297" slot was milled at this point to relieve the stress.

Light guides were twisted-strip adiabatic light guides made from five strips of 3/16" BC-800 UVT acrylic cut to about 8.8" in length. The light guides were glued to the scintillators with Dymax [2] UV curing glue and were adhered to the PMT faces with flexible plastic "cookies" provided by Bicron. The scintillators and light guides were wrapped in aluminum foil and black electrical tape. The completed Start Counter is shown in figure 3.

4 Bench tests

The performance of the three coupled paddles were bench tested using a ^{106}Ru beta source. The details of the test are given in reference [4]. The variables

[1] Bicron Corporation, 12345 Kinsman Road, Newbury, OH 44065-9677.
[2] Dymax Corporation, 51 Greenwoods Rd., Torrington, CT 06790.

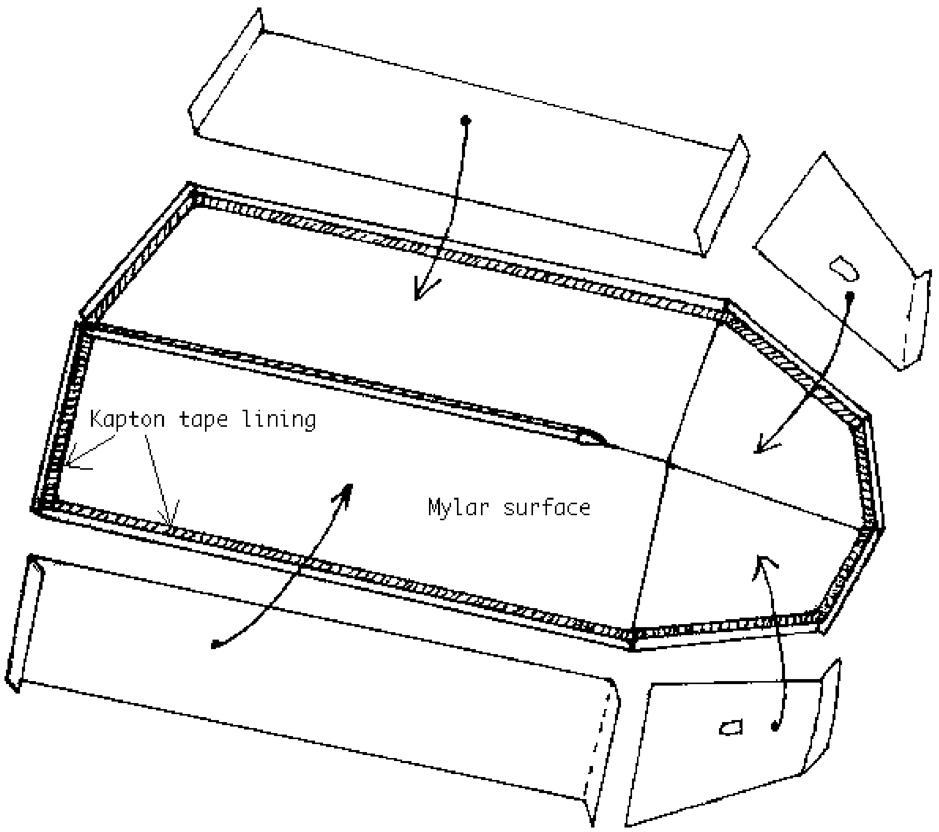

Fig. 2. Sketch of the bending fixture.

T_A and T_B refer to the TDC value for tube A and tube B, respectively. The average of the two PMT timing signals minus the jitter in the start time was calculated according to the formula

$$T_{AV}(\text{Tubes A \& B}) = \frac{T_A + T_B}{2} - T_{TRIG}. \tag{1}$$

The time jitter of the trigger was estimated to be $\sigma = 70$ ps [7]. T_A and T_B were corrected for slewing by applying the following formula on an event by

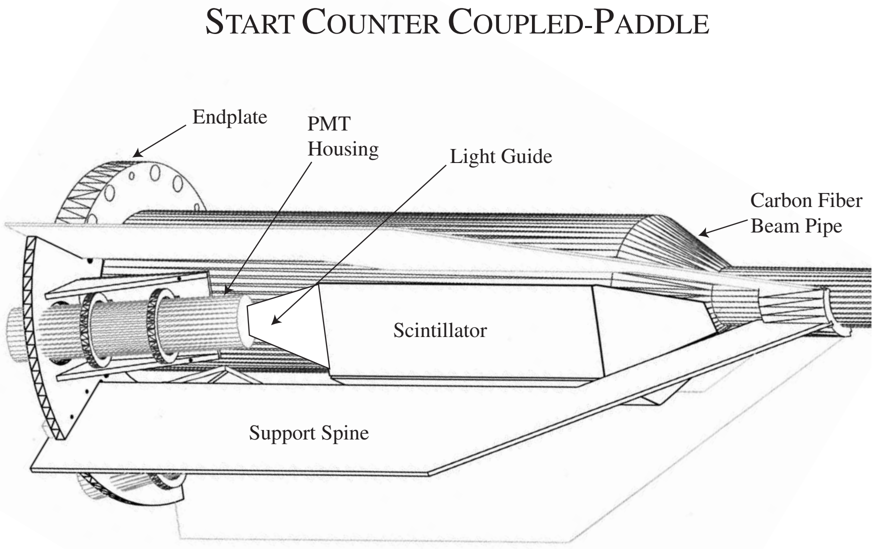

Fig. 3. Sketch of one of the completed Start Counter segments.

event basis:

$$T' = T - K\left(\frac{1}{\sqrt{A_0}} - \frac{1}{\sqrt{A}}\right), \qquad (2)$$

where T is the measured time, A_0 is the peak of the ADC spectrum, A is the measured pulse height, and K is a constant that was adjusted to minimize the timing resolution. The test data are summarized in table 1. Position A refers to the source placed near Tube A and position B refers to the source positioned near Tube B.

Table 1
Start Counter test data. The "Tail" is the fraction of events for which the measured time differed from the true time by more than 1 ns.

Scintillator	Position A σ(ps)	Tail (%)	Position B σ(ps)	Tail (%)	Nose σ(ps)	Tail (%)
1	325	1.9	355	2.8	245	1.0
2	365	4.1	360	2.3	260	1.2
3	360	3.3	370	2.7	270	1.0

5 Trigger logic

The trigger electronics must provide reliable hardware time to be used in coincidence with the tagger signal and uniform energy threshold for good background rejection. In this section we concentrate on timing achieved in hardware coincidence circuits only, but note that the best estimate of the interaction time of the photon in the target will be determined in software, off-line. Normally, double-ended scintillators achieve this by requiring a coincidence of the signals from each tube ("Logic AND mode"). In the present coupled-paddle design, the pulse height varies by a factor of five from end to the other. The loss in pulse height occurs mainly at the bends, as will be demonstrated later. Better performance can be achieved by combining the signals in an analog sum and then discriminating. The pulse heights for tubes A and B and the analog sum versus position are shown in figure 4. An exponential attenuation was assumed for simplicity. The signal from the tube nearest to the interaction dominates, and a much higher threshold (a) may be used than in the Logic AND mode (c). This is still superior to the simpler Logic OR circuit with the threshold at b, because for interactions in the "nose region" the light must travel through one bend to reach one tube and two bends to reach the other. The summed light is greater than the light from one tube alone.

To reduce the accidentals, a tight timing coincidence between the Start Counter and the tagging system is desired. Referring to figure 4 we can see that for the Analog sum there will be a region around x = 0 (forward direction) for which the pulses will not cross the threshold until both PMT signals arrive. Therefore the timing will be comparable to the Logic AND timing, if the discriminator level is set to $< b$. On the other hand the analog sum efficiency will be preserved throughout the scintillator length if the discriminator level is set to $a = 2b$. The solution chosen was to use the analog sum signal into a dual level discriminator with an upper-level threshold $ULT = 2b$ and a lower-level threshold $LLT = b$.

A schematic diagram of the trigger electronics using this scheme is shown in figure 5. Signals from each side of each paddle were summed by a Phillips

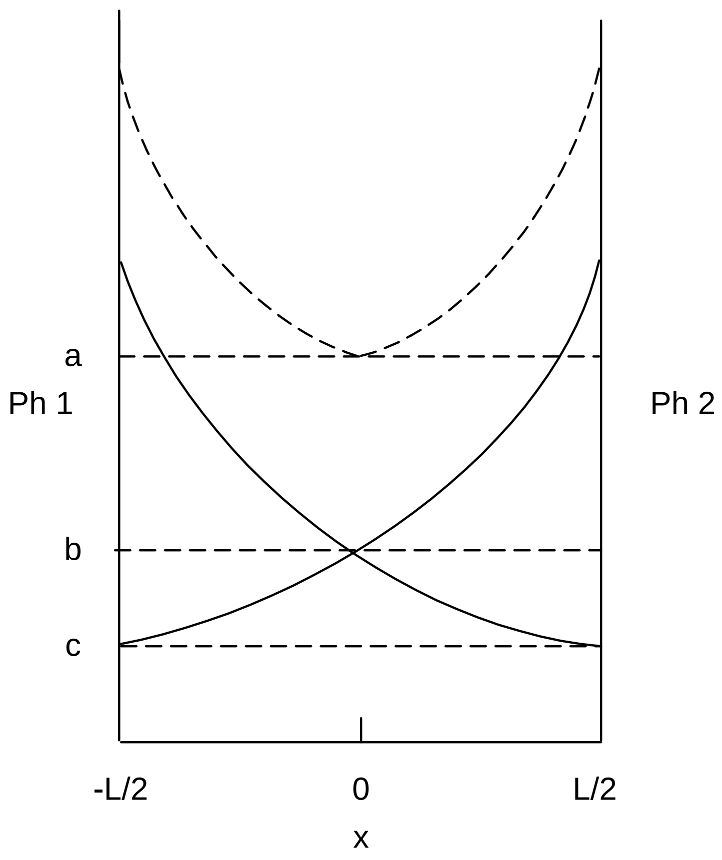

Fig. 4. Pulse height for tube 1 and tube 2 (solid curves) and the analog sum (dashed curve) versus position along scintillator. The threshold settings for the three methods of combining the tube 1 and tube 2 pulse heights are shown as dotted lines labeled a (analog sum), b (logic OR), and c (logic AND). L is the distance between the PMTs along the direction of light propagation.

Model 740 NIM Quad Linear/Logic Fan-In/Out and the resulting signal discriminated by a Philips Model 730 NIM Tri-Mode discriminator set to the ARC (Amplitude Rise-time Compensated) mode. The ARC mode is a dual level discrimination technique whereby a logic pulse is produced only if the input signal exceeds an upper-level threshold (ULT) but whose timing is dictated by a lower-level threshold (LLT). The LLT was set to 65 mV, just above the noise level of the summed signals; the ULT was set to 130 mV, to yield good efficiency. Finally, the logic pulses from each discriminator were OR'ed together to provide the Start Counter trigger signal. The width was set to 15 ns. This width was chosen to be fully efficient to include all data, including slow particles, from three beam buckets, so that accidentals in the data sample could be accurately subtracted later. The trigger for an event in CLAS was formed from a coincidence between the Start Counter signal, the OR of all the signals from the T-counters, and the OR of the signals from the Time-of-flight.

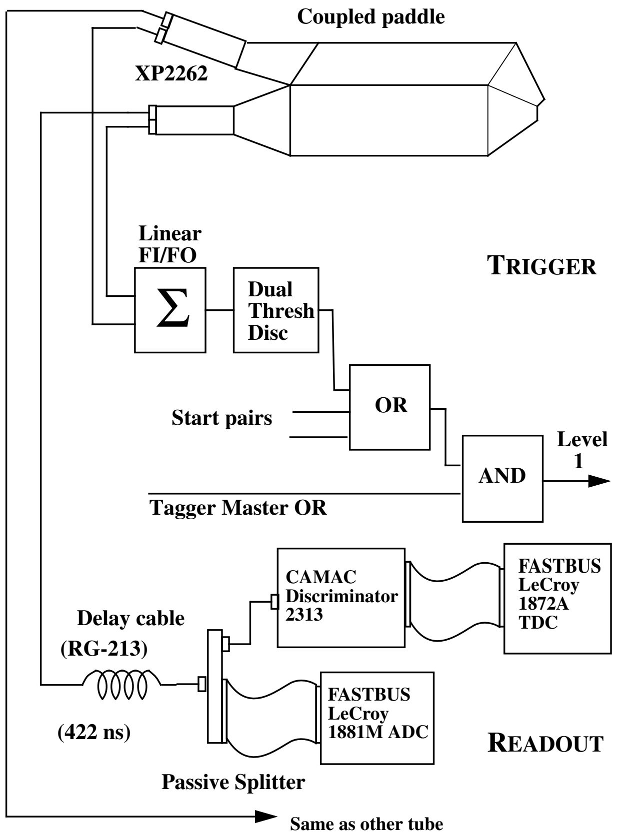

Fig. 5. Schematic diagram of the trigger and readout electronics.

A second signal from each of the six tubes was fed into a passive splitter. Eighty percent of the signal was passed to a LeCroy 2313 leading-edge discriminator. The timing information was read out with a LeCroy 1872-mod 100 TDC. The remaining 20% was passed to a LeCroy 1881M ADC for pulse height measurement. A schematic diagram of the readout electronics is shown in figure 5.

6 Performance

The Start Counter was installed in CLAS in April 1998 for a commissioning run using a bremsstrahlung photon beam with energies between 0.2 E_0 and 0.95 E_0, where E_0=2.5 GeV is the energy of the primary electron beam. Figure 6 shows the trigger timing, which is the Start counter timing with respect to the tagger time. The timing has not been corrected for transit time or position. As can be seen from the figure, the goal of catching three beam buckets to measure accidentals was successful. Figure 7 shows the pulse height in Tube A versus the pulse height in Tube B. The distinctive pattern can be understood by considering the three regions of the paddle. The side lobes are due to the case where the particle hit near tube A (vertical lobe) or near tube B (horizontal lobe). The central lobe is due to particles that hit in the "nose" region where both tubes collect about the same amount of light. This implies, not surprisingly, that the light loss going from Tube A to Tube B has a sharp drop-off as one goes through the nose region. Figure 8 shows the pulse height versus the position along the scintillator for a single track in the hit paddle. The sharp drop in pulse height near 22 cm corresponds to the 30° bend of the scintillator. These data have a valid hit and track in another Start Counter paddle and thus is a measure of the trigger efficiency. The hardware threshold is set to about 125 channels so that the Start Counter is highly efficient.

Figure 9 shows the time versus position in the two legs of a Start Counter paddle. The time has been corrected for pulse height (slewing) and for the transit time of the particle from the interaction point to the scintillator. The slope of this curve gives the effective velocity of the light in the scintillator. The value for the light going to the nearest tube is approximately 13 cm/ns. It is close to the velocity of light in the bulk material traveling at the critical angle. The velocity of the light traveling to the farthest tube is considerably faster. This can be explained by two effects, the path length around the bend is not well defined and may be shorter than the distance used (a straight line from the tube to the end of the scintillator) and the fact that only a small portion of the light makes it around the bent portion of the scintillator. This light must necessarily occupy a smaller phase space than the light going to the nearest tube. The most likely parts of phase space to be lost in the bends are the light at the largest angle. Ultimately only the most direct light will make it, giving a substantially faster effective velocity. This complicates the calculation of the interaction time. The standard double ended equation assumes equal pulse heights and transit times. If the time resolution is dominated by photon statistics, the time resolution of the far tube is more than a factor of two worse than the near tube timing resolution. Furthermore the different travel times result in a position-sensitive mean time. Specifically,

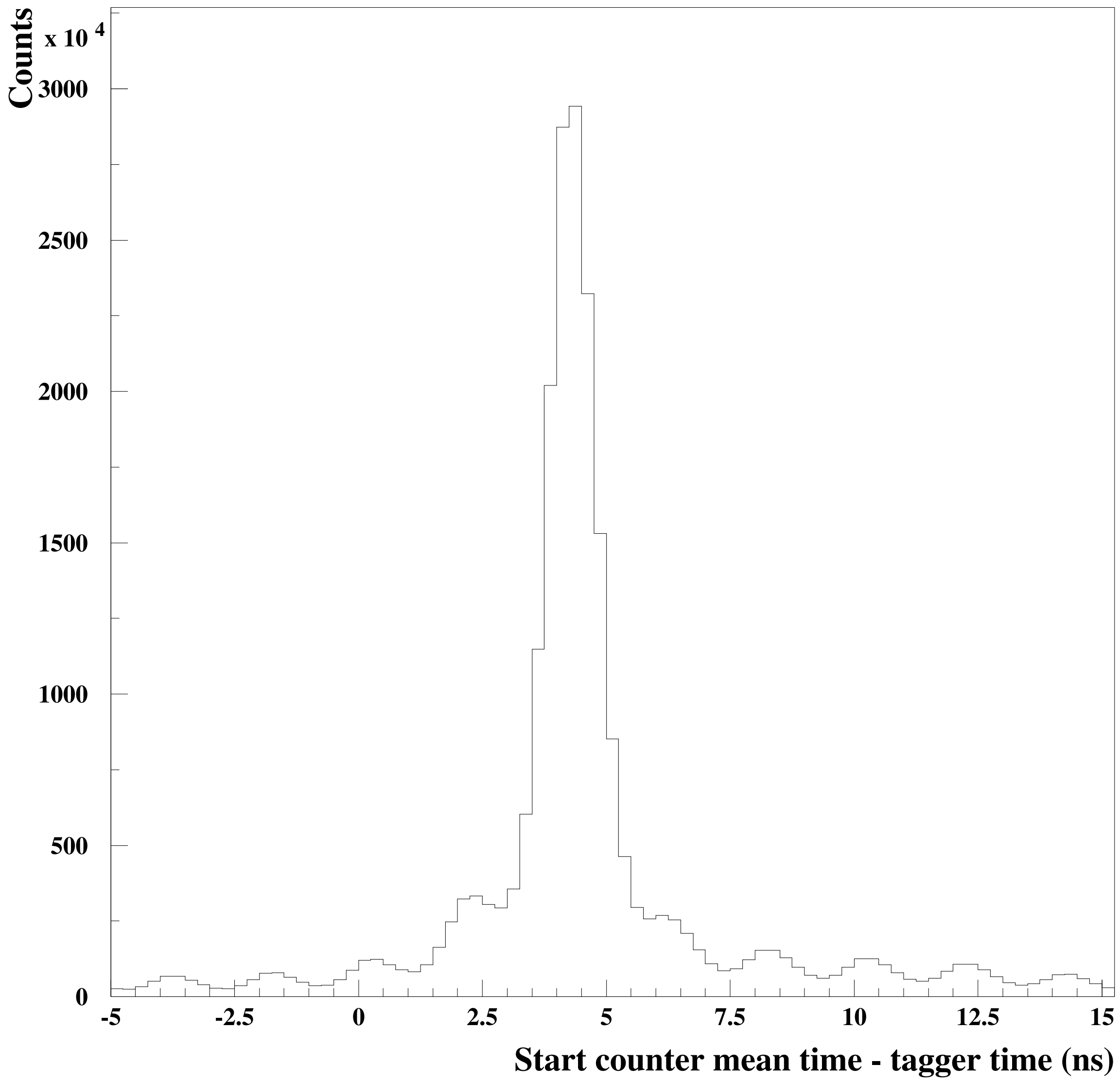

Fig. 6. Start Counter trigger timing relative to the tagger. No correction has been made for hit position.

$$T_A + T_B = T_0 + \frac{x}{v_1} + T_0 + \frac{L-x}{v_2} \tag{3}$$

$$T_0 = \frac{T_A + T_B}{2} - \frac{L}{2v_2} - \frac{x(v_2 - v_1)}{2v_1 v_2}, \tag{4}$$

where x varies from 0 to L/2. For $x > L/2$ tube A and tube B switch their meaning. For $v_1 = 13$ cm/ns, $v_2 = 17$ cm/ns and $\Delta x = 50$ cm we get a spread

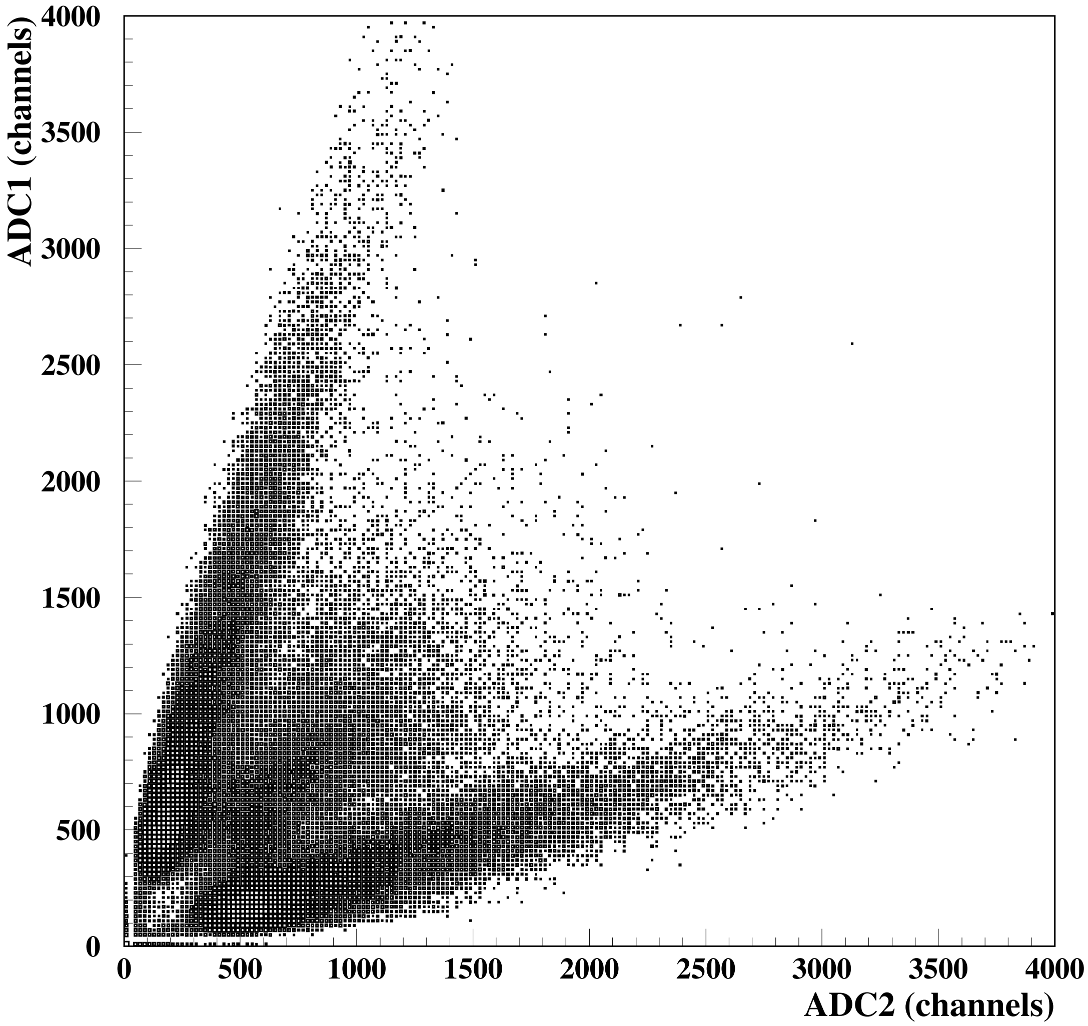

Fig. 7. Pulse height in Tube A (ADC1) plotted against pulse height in Tube B (ADC2) for one of the coupled paddles.

of 0.9 ns.

Therefore to get the ultimate timing resolution we use a weighted average and make a position dependent correction to calculate the mean time.

$$T_0 = \frac{AT_A + BT_B}{A+B} - \frac{BL}{(A+B)v_2} - \frac{x(Av_2 - Bv_1)}{(A+B)v_1 v_2}. \tag{5}$$

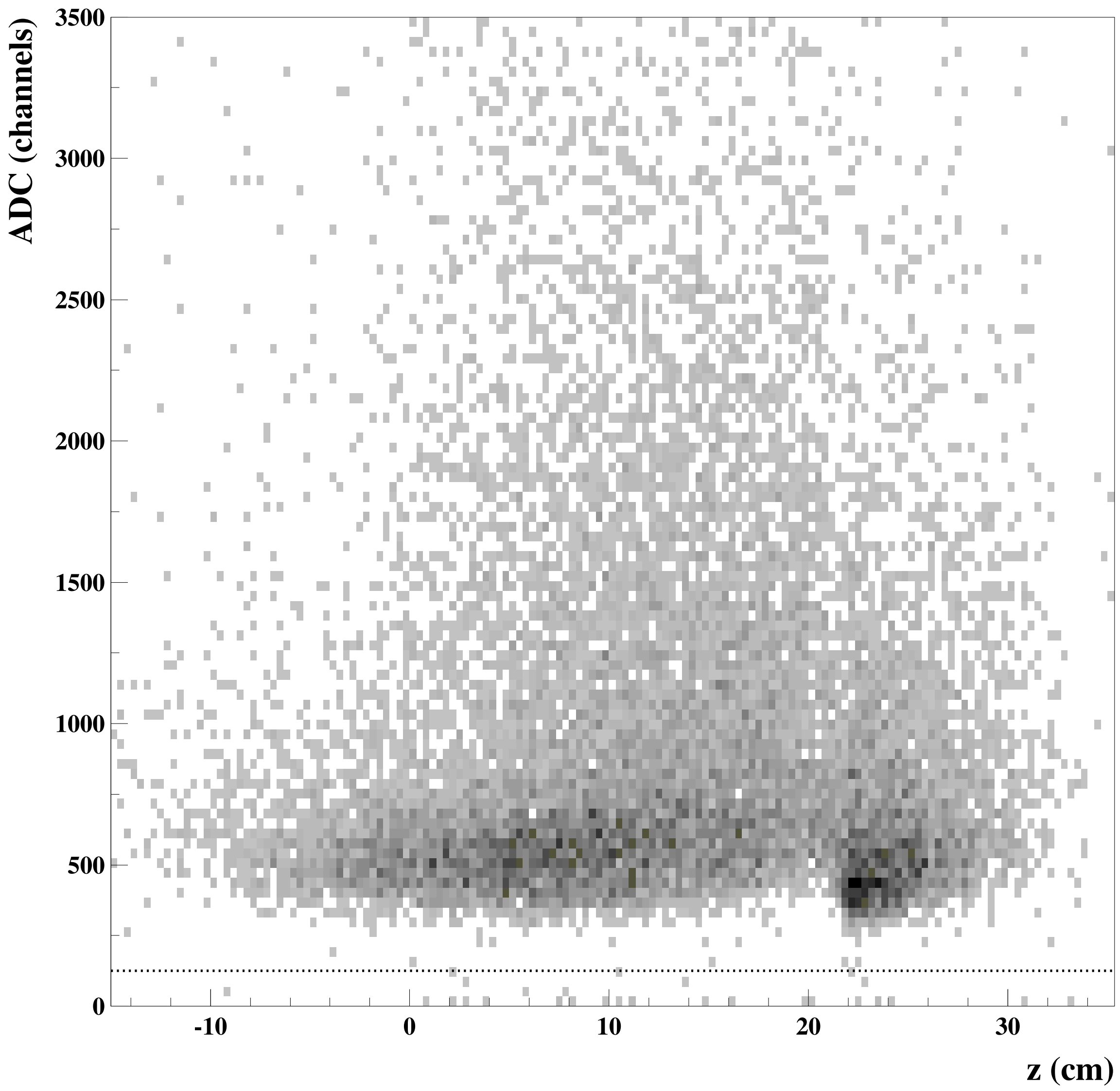

Fig. 8. Pulse height as a function of position along the beam direction for the case where a single track hit the pair for one of the three pairs. The dotted line is the hardware threshold (125 channels).

Here A is the pulse height from tube A and B is the pulse height from tube B, v_1 is the velocity to the nearest tube and v_2 is the velocity to the farthest tube. The position x is determined independently using the tracking information from the drift chambers. This equation is valid for $0 < x < L/2$. Assuming that the time resolution is limited by photostatistics, the weighted-average time resolution can be computed in terms of σ_0, the time resolution from a

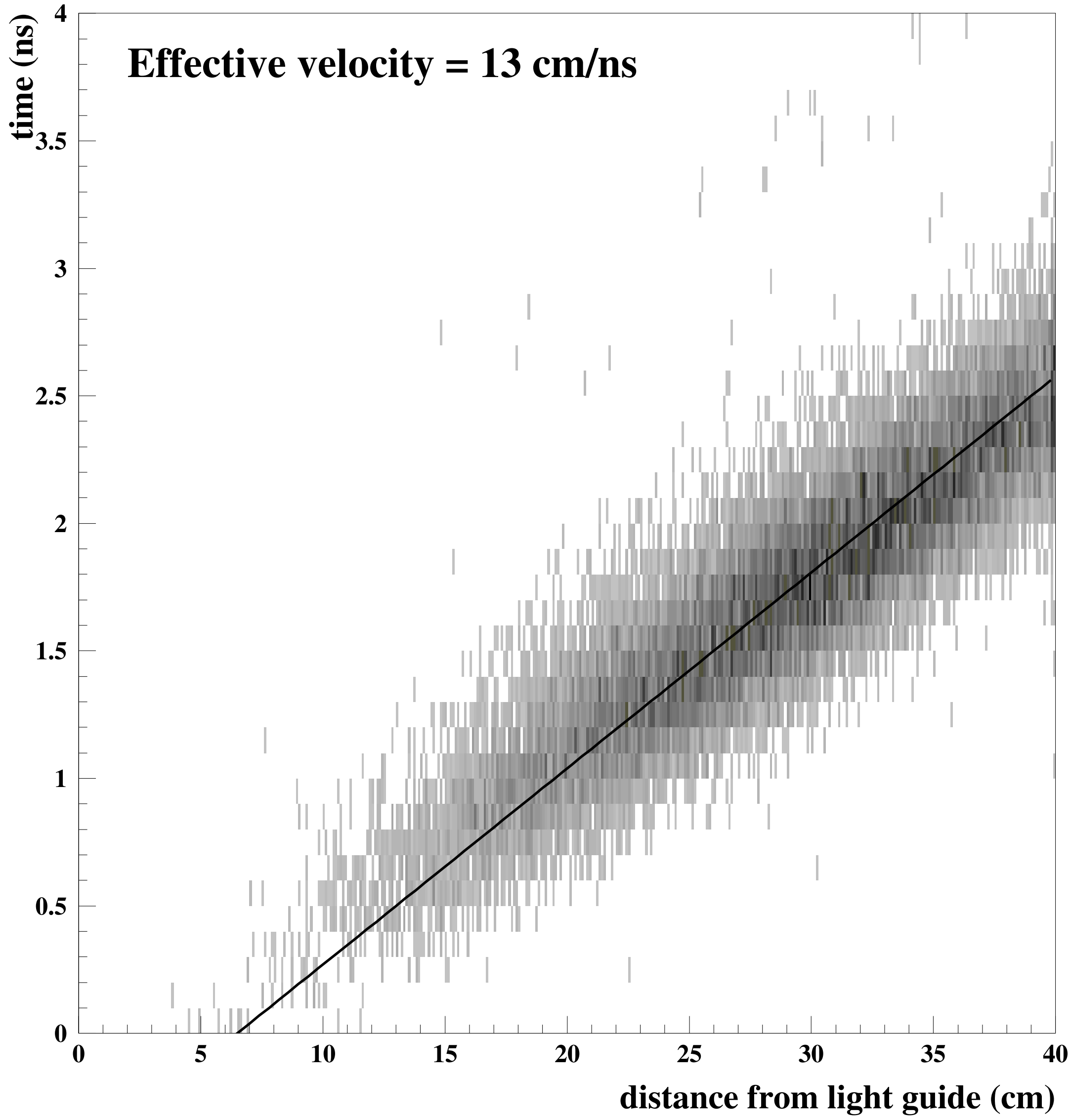

Fig. 9. Determination of the velocity of propagation for light going to the nearest PMT. The z-position is determined by tracks reconstructed by the CLAS tracking system.

minimum ionizing pulse in the leg near the tube. Then the time resolution is given by

$$\Delta T = \sqrt{\frac{(A\sigma_A)^2 + (B\sigma_B)^2}{(A+B)^2}}. \tag{6}$$

Table 2
Comparison of timing methods for π^+ particles passing through each of the three scintillators near one of the tubes. The resolution is given for each of the six sectors in the CLAS detector.

		Sector					
Timing method		1	2	3	4	5	6
Mean time	σ_a (ps)	377	415	282	347	325	306
Weighted Average	σ_w (ps)	263	269	249	242	252	254
Nearest tube	σ_0 (ps)	303	270	270	260	269	296
	$\frac{\sigma_a}{\sigma_0}$	1.24	1.54	1.04	1.33	1.21	1.03
	$\frac{\sigma_w}{\sigma_0}$	0.87	1.00	0.92	0.93	0.94	0.86

If we set $f = A/B$ and $\sigma_B = \sqrt{f}\sigma_A$, we get

$$\Delta T = \sigma_0 \sqrt{\frac{f}{1+f}}, \tag{7}$$

where we have ignored errors due to uncertainty in the position of the hit and the uncorrelated variation of the pulse height due to the PMT gains. A single-ended paddle would have $\Delta T = \sigma_0$. For $f = 5$ we get $\Delta T = 1.23\sigma_0$ for the mean time and $\Delta T = 0.93\sigma_0$ for the weighted average. These all assume that the position dependent correction has been made with little or no error. Thus we conclude that the mean time gives the best timing for $f < 2$, the weighted average is best for $2 < f < 10$, and using the nearest tube is best for large f. Table 2 shows the time resolution for these three cases for the three paddles. In each case the results are shown for only one hit in the paddle. Backward-going π^+ particles (i.e., particles traversing the leg portion of the paddle) were chosen for the comparison. As expected, the mean time has the worst resolution and the weighted-average generally gives the best timing. From Table 2, we see that an average of the Mean time is $1.23\sigma_0$ and an average of the Weighted time is $0.92\sigma_0$, in agreement with a value of $f = 5$.

If there are more than one hit in a paddle, the situation is much more complicated. If the hits are in opposite legs, then the closest tube is the best choice, while if the two hits are in the same leg, or both in the nose, then the situation is ambiguous. Using the mean time may be best. Figure 10 shows these cases. For the case (figure 10A) where a single charged particle strikes a paddle, the fraction of counts that fall outside of a ± 1 ns window about the centroid is about 0.01%. For cases 10B and 10C, this fraction is less than 2.3% and 4.1%, respectively. These fractions may include accidental hits in adjacent beam buckets, so they correspond to upper limits.

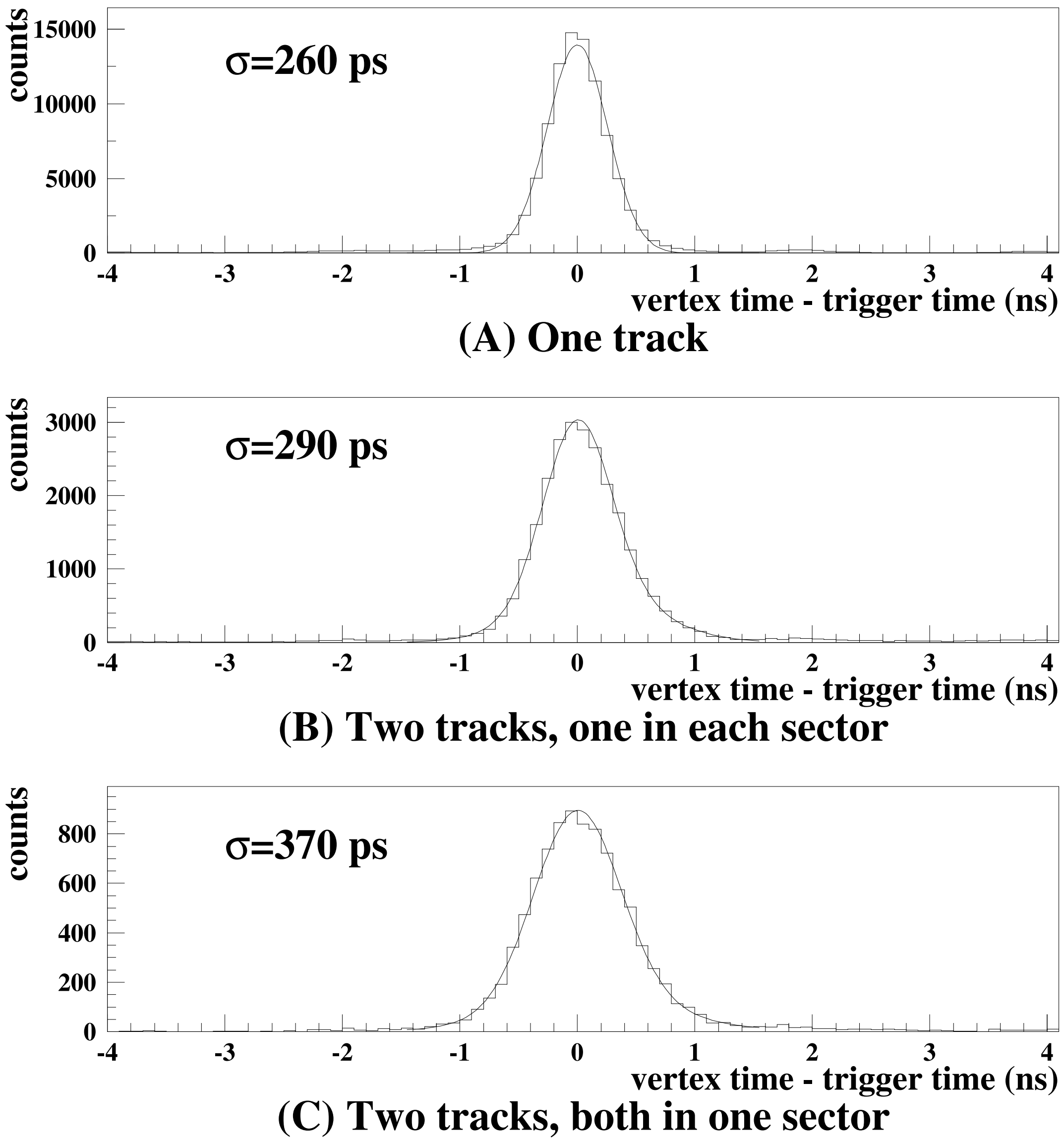

Fig. 10. Start Counter timing for (A) one track in a paddle; (B) two tracks, one in each sector for a single paddle; and (C) two tracks, both in the same sector for a single paddle. A single gaussian was used to fit (A). Two gaussians were used to fit (B) and (C); the resolution quoted is the standard deviation of the dominant gaussian. Note that the tails of the distributions increase for events with two tracks.

7 Discussion and conclusion

A coupled paddle design for the CLAS Start Counter was built and tested. Bench tests with a ^{106}Ru beta source show that for charged particles interacting near one PMT, the far PMT sees approximately 20% of the pulse height of the near tube.

The counter was installed in the CLAS detector and performed well. The measured time resolution ranges from 255 ps (for pulses in the "nose" region which are viewed equally well by both tubes), to 271 ps (for pulses near one tube) with an average of about 260 ps for the case where only one track strikes a given scintillator. The average value is weighted towards the nose region due to the cross section. The times quoted have been corrected for pulse height slewing and particle flight time. Comparison of extrapolated tracks from the DC's with the pulse height seen in each paddle for hits in more than one sector, clearly demonstrate that the goal of ∼100% efficiency was achieved. The identification of the beam bucket associated with a given event could be achieved to the desired level. However, the detector could only achieve its performance goals at or below a singles rate of about 1.2 MHz per paddle. At an order-of-magnitude above this rate the accidental coincidences with the tagger made it impossible to uniquely associate a given charged particle in CLAS with a given tagger event. In such a situation a single paddle design may be preferable.

Since the coupled paddle design leads to a position dependent time, and a time resolution only about 10% better than a single paddle design one might consider using six single ended paddles. Such a configuration has two very strong points to recommend it. The first is reduced accidentals. The individual rate in each paddle will be halved, allowing for the possibility of reducing the accidentals. The second is ease of construction. Only one bend is required, the 30° bend near the nose. Without a double-ended paddle, however, one cannot get a hardware mean time, which even in the coupled paddle design gives a time spread (FWHM) of less than 1.25 ns. The single-ended trigger time for a single paddle was estimated by taking only those events that hit in one leg of the coupled paddle and using the time for tube attached to that leg. The spread (FWHM) for this case was about 3 ns.

Acknowledgements

The authors would like to thank Harry Themann for preparing the mechanical drawings of the bending fixtures, King Yee Chan for his invaluable help in the construction of the final detector, and John Ficenec for helpful suggestions during the writing of this article.

References

[1] B. Mecking *et al.*, in preparation.

[2] D. I. Sober *et al.*, Nucl. Instrum. Meth. **A440/2**, 263-284 (2000).

[3] E. S. Smith *et al.*, Nucl. Instrum. Meth. **A432**, 265 (1999).

[4] S. Taylor, "Scintillation Detector Development for the Solenoidal Tracker at RHIC (STAR) and the CEBAF Large Acceptance Spectrometer (CLAS)", Master's Thesis, Rice University, 1996.

[5] T. Smith, J. Distelbrink, and G. Briggs, "A 'Coupled-Paddle' Design for the Start Counter of CLAS", CLAS-NOTE 94-003.

[6] T. Massam, "Guide 7: A General Program For Evaluating The Properties Of Scintillation And Cerenkov Counter Optical Systems," CERN 76-21.

[7] S. Ahmad, B. E. Bonner, W. Gere, G. S. Mutchler, P. Rambo, S. Toshkov, E. Platner, H. J. Crawford, and J. M. Engelege, Nucl. Instrum. Meth. **A330**, 416 (1993).